

We are IntechOpen, the world's leading publisher of Open Access books Built by scientists, for scientists

4,800

Open access books available

122,000

International authors and editors

135M

Downloads

Our authors are among the

154

Countries delivered to

TOP 1%

most cited scientists

12.2%

Contributors from top 500 universities



WEB OF SCIENCE™

Selection of our books indexed in the Book Citation Index
in Web of Science™ Core Collection (BKCI)

Interested in publishing with us?
Contact book.department@intechopen.com

Numbers displayed above are based on latest data collected.
For more information visit www.intechopen.com



Corrosion Protection of Magnesium Alloys in Industrial Solutions

Amany Mohamed Fekry

Additional information is available at the end of the chapter

<http://dx.doi.org/10.5772/58942>

1. Introduction

The main problem in our life is the corrosion of many types of alloys either industrially or biologically. This work reviews the corrosion protection of magnesium based alloys in industrial solutions. Corrosion behavior had been studied using electrochemical impedance spectroscopy (EIS), Potentiondynamic polarization and scanning electron microscope (SEM) techniques. Magnesium is the lightest of all metals in practical use with density of 1.74 g cm^{-3} . Pure magnesium metal has useful properties such as shielding against electromagnetic waves, vibration damping, dent resistance and machinability, in addition to its recyclability as it has a lower specific heat and a lower melting point than other metals. On the other hand, magnesium has shortcomings such as insufficient strength, elongation and heat resistance as well as being subject to corrosion. It is necessary to deal with its shortcomings and improve its performance through alloying with various elements. Alloying magnesium improves its strength, heat resistance and creep resistance [1].

Magnesium alloys are the most versatile and attractive metallic materials. They are used for a broad range in commercial, industrial and aerospace applications due to their many advantages, such as light density, good mechanical properties and excellent castability [2-4]. The most common magnesium alloys are those containing aluminum, Zinc, manganese, zirconium, thorium and rare earth metals. The latter alloys are used when resistance to creep and high temperature strength are required. One of the major problems that limit magnesium alloys application is their high susceptibility to corrosion in different media [5] which depends widely on film formation and surface electrolyte interaction. A serious limitation for the wide-spread use of several magnesium alloys is their susceptibility to general and localized (pitting) corrosion. The AZ-based Mg system has been the basis of the most widely used magnesium alloys [6]. One of the most successful magnesium-aluminium alloy is AZ91D, which has a two-

phase microstructure typically consisting of α -Mg matrix with the β -phase (the intermetallic $\text{Mg}_{17}\text{Al}_{12}$) distributed along the α grain boundaries. The α -phase consists of α -Mg-Al-Zn solid solution with the same structure as pure magnesium [5]. Also AZ31E alloy have excellent mechanical properties. Extruded Mg alloys as AZ31E is getting more and more widely used because of their considerably high plasticity in comparison with the die-cast Mg alloys [7].

Corrosion is a major problem in the cooling system of an engine block. Currently, the main composition of a conventional coolant is 30–70 vol% ethylene glycol [7]. This can be used for studying the corrosion behavior of AZ91D alloy. Most existing commercial coolants fail to provide adequate corrosion protection to magnesium alloys [8]. Some companies have also realized the difficulty of using the conventional coolants for magnesium alloys, and are developing coolants with new inhibitors [9]. Song et al. [7] observed that the corrosion rate of magnesium in aqueous ethylene glycol depends on the concentration of the solution. A diluted ethylene glycol solution is more corrosive than a concentrated one at room temperature. Ethylene glycol solution contaminated by individual contaminants NaCl, NaHCO_3 or Na_2SO_4 is more corrosive to magnesium. NaCl is the most detrimental contaminant. In this work, a study for the corrosion behavior of AZ91D alloy in this coolant has been done, due to this issue is important industrially. The aim is to characterize the corrosion properties of AZ91D alloy in aqueous ethylene glycol-water solutions of different percentages. The influence of adding chloride or fluoride ion in ethylene glycol solution on the corrosion behavior was studied. Also the effect of paracetamol ((N-acetyl-para-aminophenol=APAP) as inhibitor in ethylene glycol for AZ91D alloy is investigated [6].

Electrochemical characterization and corrosion behavior of AZ31E alloy was done in aqueous Oxalic acid as industrial solution [10]. Oxalic acid is a relatively strong organic acid used as purifying agent in pharmaceutical industry. Oxalic acid's main applications include cleaning or bleaching, especially for the removal of rust [11]. The work aims to attain more information concerning the corrosion behavior of AZ31E alloy in oxalic acid solution containing Cl⁻, F⁻ or PO_4^{3-} anions under various environmental conditions. The corrosion rate was found to increase with increasing oxalic acid concentration. The effect of adding Cl⁻, F⁻ or PO_4^{3-} ions on the electrochemical behavior of AZ31E electrode was studied in 0.01 M oxalic acid solution at 298 K. It was found that the corrosion rate increases with increasing Cl⁻ or F⁻ ion concentration, however, it decreases with increasing PO_4^{3-} ion concentration [12].

2. The main problem

One of the major problems that limit magnesium alloys application is their high susceptibility to corrosion in different media. This makes studying the corrosion and corrosion control of Mg alloys an interesting point of research which can enable extending the potential use of these important materials in a broad range of many technical and innovative applications.

3. The aim

The aim is to study the corrosion resistance of Mg alloys which depends essentially on two main factors: (i) alloy microstructure and (ii) properties of the developed surface film.

Generally, it is aimed to find the best magnesium alloy with low cost and low corrosion rate and to find a possible way to improve corrosion resistance of either AZ91D or AZ31E alloy in different industrial solutions.

4. Experimental

Samples of die cast magnesium aluminum alloy (AZ91D or AZ31E) in the form of plates (200 x 100 x 5 mm) were donated from Department of mining, Metallurgy and Materials Engineering, Laval University, Canada. The chemical composition (wt%) of the two alloys are as follows: 9.0 Al, 0.67 Zn, 0.33 Mn, 0.03 Cu, 0.01 Si, 0.005 Fe, 0.002 Ni, 0.0008 Be and balance Mg for AZ91D alloy; and 2.8 Al, 0.96 Zn, 0.28 Mn, 0.0017 Cu, 0.0111 Fe, 0.0007 Ni, 0.0001 Be and balance Mg for AZ31E. They were used for preparing the working electrodes. The sample was divided into small coupons. Each coupon was welded to an electrical wire and fixed with Araldite epoxy resin in a glass tube leaving cross-sectional area of the specimen 0.2 cm² for AZ91D alloy and 0.196 cm² for both AZ31E alloy.

The solutions used were prepared using Analar grade reagents for each work are (ethylene glycol, sodium fluoride, sodium chloride and paracetamol [6]) and (oxalic acid, sodium fluoride, sodium chloride and sodium phosphate [12]). All solutions were prepared using triply distilled water.

The surface of the test electrode was mechanically polished by emery papers with 400 up to 1000 grit to ensure the same surface roughness, degreasing in acetone, rinsing with ethanol and drying in air.

The cell used was a typical three-electrode one fitted with a large platinum sheet of size 15×20×2mm as a counter electrode (CE), saturated calomel (SCE) as a reference electrode (RE) and the alloy as the working electrode (WE).

The impedance diagrams were recorded at the free immersion potential (OCP) by applying a 10 mV sinusoidal potential through a frequency domain from 100 kHz down to 100 mHz. The EIS was recorded after reading a steady state open-circuit potential. The polarization scans were carried out at a rate of 1 mV/s over the potential range from -2.5 to 0 mV vs. saturated calomel electrode (SCE). Prior to the potential sweep, the electrode was left under open-circuit in the respective solution until a steady free corrosion potential was recorded. Corrosion current, i_{corr} , which is equivalent to the corrosion rate is given by the intersection of the Tafel lines extrapolation. In the weight loss measurements, the treated samples were weighed before and after the immersion in Hank's solution in absence and in presence of different concentrations of glucosamine sulphate. The instrument used is the electrochemical workstation IM6e

Zahner-elektrik, GmbH, (Kronach, Germany). The electrochemical and weight loss experiments were always carried inside an air thermostat which was kept at 25°C, unless otherwise stated. The SEM micrographs were collected using a JEOL JXA-840A electron probe micro-analyzer.

5. Results and discussion

5.1. Electrochemical impedance measurements

5.1.1. AZ91D alloy in ethylene glycol solution [6]

The EIS scans of AZ91D alloy as a function of concentration for ethylene glycol were recorded (Figure 1) after leaving the working electrode for 2 h in the test solution until reaching a steady state potential value (E_{st}). As shown in Figure 1, an increase in ethylene glycol concentration leads to a decrease in the $|Z|$ value, indicating that pure ethylene glycol is almost inert to magnesium alloy and the corrosion of magnesium alloy in ethylene glycol solution is closely related to the water content of the solution [7].

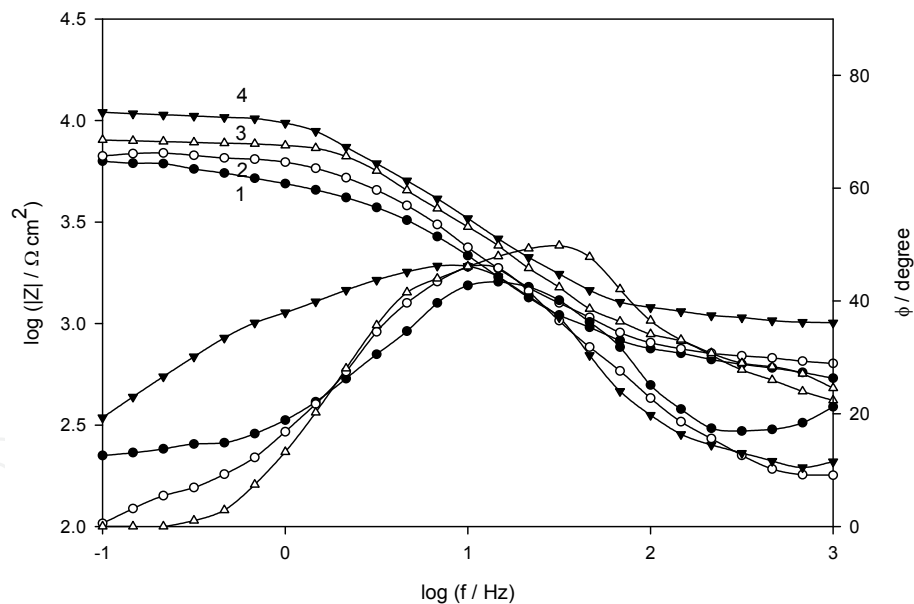


Figure 1. EIS data of AZ91D alloy exposed after 2 h immersion in various concentrations of ethylene glycol solution: (1) 30%, (2) 50%, (3) 70% and (4) 90%.

By studying the effect of adding either fluoride or chloride to the highest corrosive concentration (30% ethylene glycol-70% water), it was found that the impedance value decreases (Figure 2a) with increasing chloride ion concentration due to its aggressiveness [10]. However, for fluoride containing ethylene glycol solution impedance value increases with increasing F^- ion concentrations shown in Figure 2b.

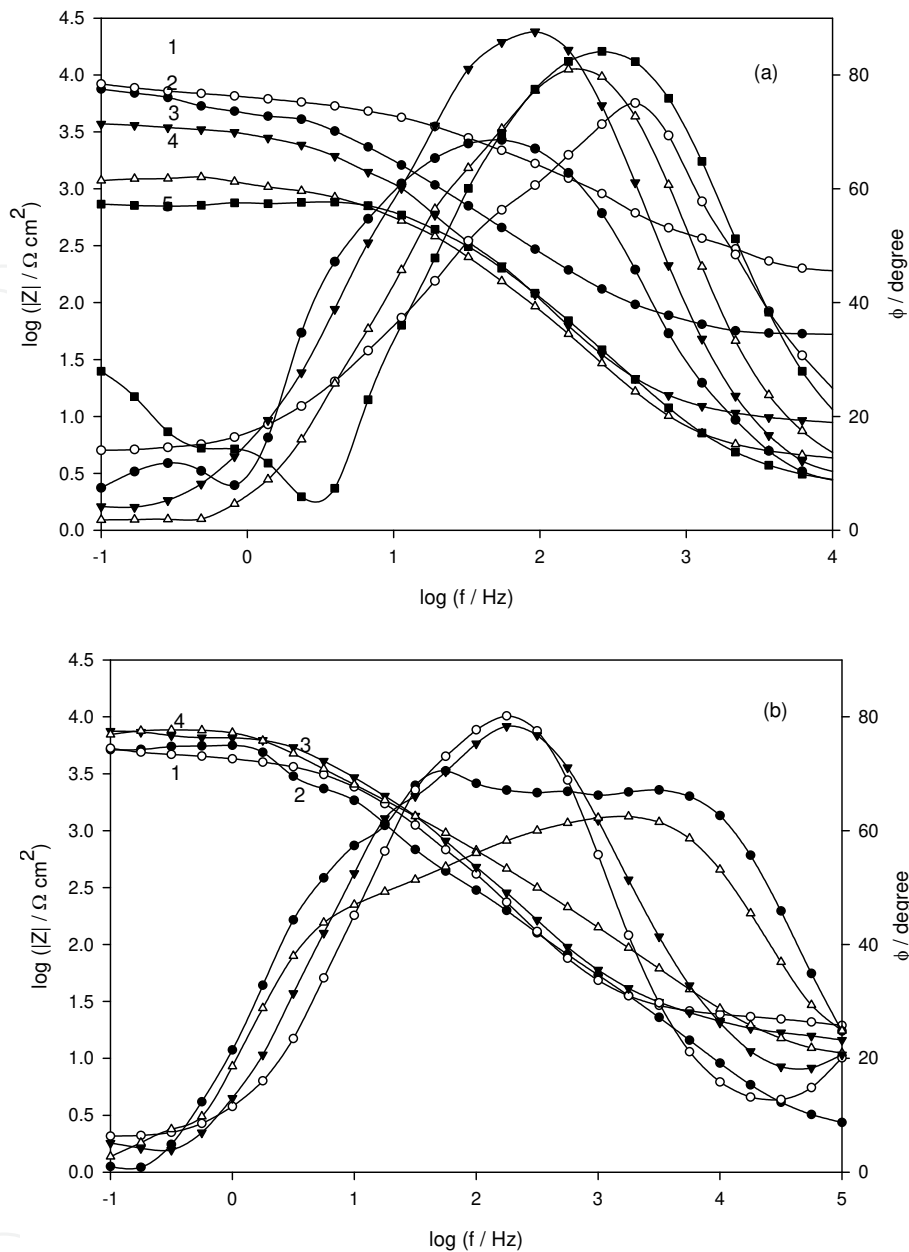


Figure 2. EIS data of AZ91D alloy exposed after 2 h immersion in 30% ethylene glycol solution with (a) chloride and (b) fluoride ions of various concentrations: (1) 0.01 M, (2) 0.05 M, (3) 0.1 M, (4) 0.3 M and (5) 0.6 M.

On adding paracetamol as inhibitor in the concentration range (0.01-1.0 mM) for corrosion of the blank (30% ethylene glycol-70% water), it was found that both $|Z|$ value and phase angle maximum (ϕ) increase suddenly up to 0.05 mM then decrease regularly up to the highest concentration of inhibitor as shown in Figure 3(a,b) as Bode and Nyquist formats, respectively.

The results in general reveal two clear trends concerning the number of peaks observed in the patterns of the phase shift. The first one is for the behavior of AZ91D alloy in chloride, fluoride and paracetamol containing ethylene glycol, where the Bode plots display only one maximum phase lag at all tested concentrations, however, for paracetamol, the phase angle maximum is

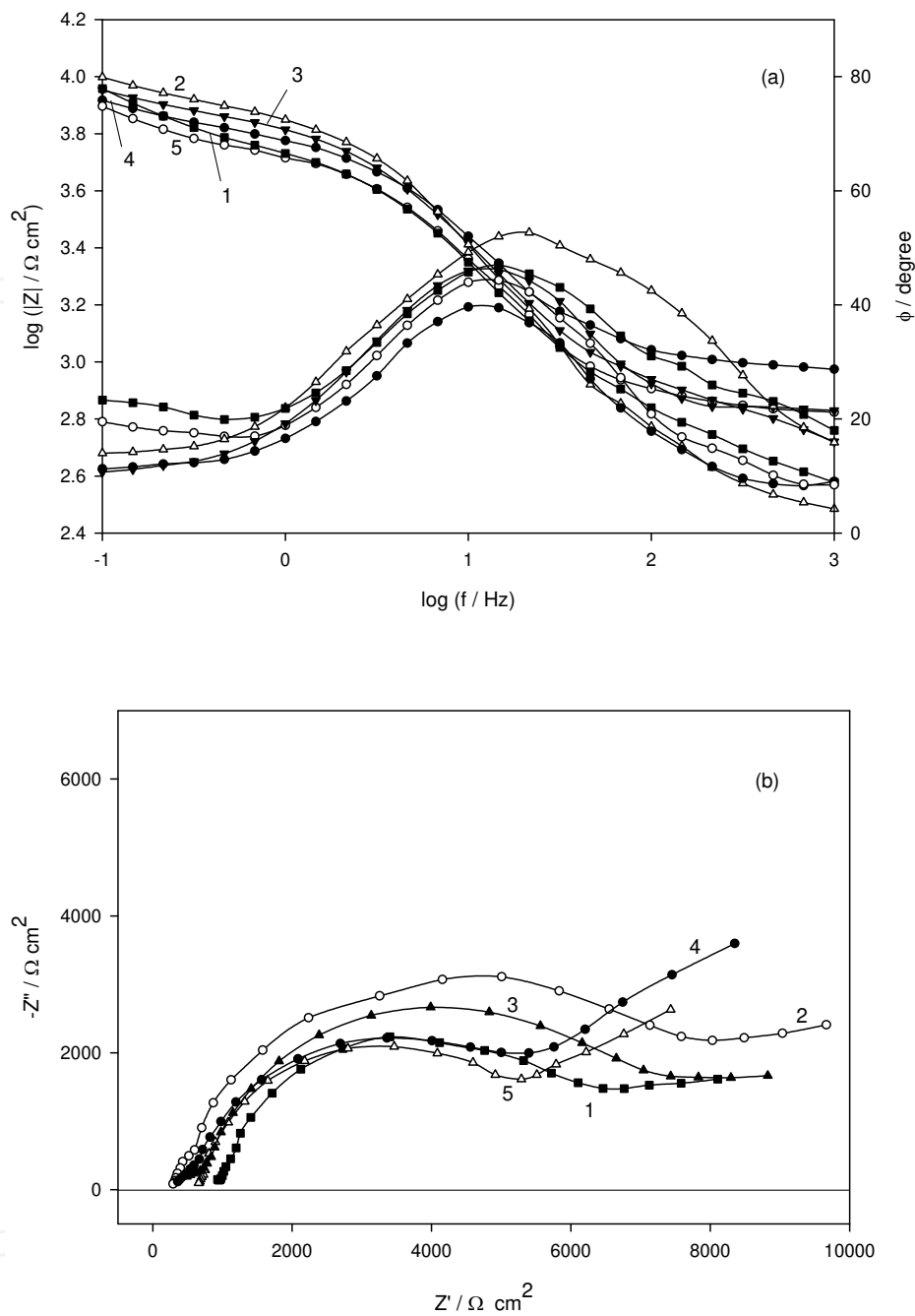


Figure 3. EIS data (a) Bode plots and (b) Nyquist plots of AZ91D alloy exposed after 2 h immersion in 30% ethylene glycol solution with paracetamol of various concentrations: (1) 0.01 mM, (2) 0.05 mM, (3) 0.1 mM, (4) 0.5 mM and (5) 1.0 mM.

nearly 45° , corresponding to a diffusion control in the passive layer. The second trend is for the alloy behavior in ethylene glycol medium with different concentrations where another peak of phase lag appears at the low frequency region and also the phase angle maximum is nearly 45° due to diffusion phenomenon. The impedance data were thus simulated to the appropriate equivalent circuit for the cases with one time constant (Figure 4a,b) and the others exhibiting two time constants (Figure 4c), respectively. This simulation gave a reasonable fit.

The estimated data for ethylene glycol is given in Table 1, for chloride and fluoride ions in Table 2 and for paracetamol ethylene glycol containing solution in Table 3.

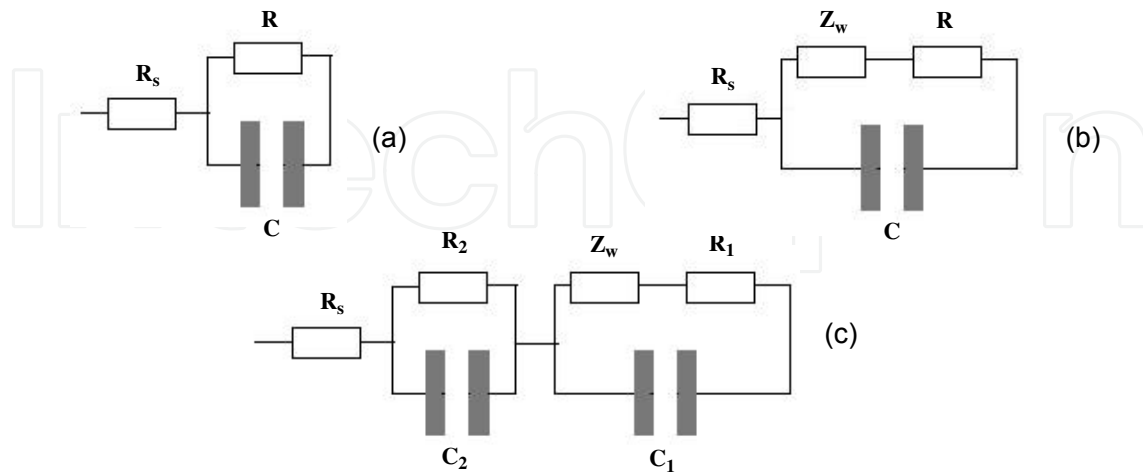


Figure 4. The equivalent circuit model representing (a,b) one and (c) two time constants.

$C_{\text{ethylene glycol}}$ (vol.%)	R_s ($\Omega \text{ cm}^2$)	R_1 ($\text{k}\Omega \text{ cm}^2$)	C_1 (nF cm^2)	R_2 ($\text{k}\Omega \text{ cm}^2$)	C_2 ($\mu\text{F cm}^2$)	W $\text{k}\Omega \text{ cm}^2 \text{ s}^{-1/2}$	R_T ($\text{k}\Omega \text{ cm}^2$)	$1/C_T$ ($\mu\text{F}^{-1} \text{ cm}^2$)	i_{corr} ($\mu\text{A cm}^{-2}$)	E_{corr} V
30	11.4	0.5	88.9	4.4	4.5	1.64	5.0	11.5	0.50	-1.45
50	21.9	0.7	77.9	6.2	4.3	1.52	6.9	13.1	0.41	-1.34
70	26.8	1.2	71.0	10.5	4.2	1.47	11.7	14.3	0.25	-1.26
90	30.0	1.4	66.4	15.4	4.0	1.33	16.8	15.3	0.1	-1.18

Table 1. Equivalent circuit and corrosion parameters for AZ91D alloy in various concentrations of ethylene glycol solution after 2 h immersion

Salt	C_{anion}	R	C	R_s	i_{corr}	E_{corr}
	(M)	($\text{k}\Omega \text{ cm}^2$)	($\mu\text{F cm}^2$)	($\Omega \text{ cm}^2$)	($\mu\text{A cm}^{-2}$)	V
NaCl	0.01	7.7	2.67	154.8	0.47	-1.36
	0.05	5.8	4.36	50.2	0.49	-1.43
	0.10	3.1	7.44	9.0	0.64	-1.52
	0.30	1.1	8.50	4.2	3.40	-1.53
	0.60	0.6	9.58	2.5	30.4	-1.63
NaF	0.01	4.1	3.54	22.1	0.19	-1.41
	0.05	5.5	3.46	21.8	0.11	-1.43
	0.10	7.0	2.46	15.8	0.09	-1.45
	0.30	8.4	1.23	7.3	0.03	-1.51

Table 2. Equivalent circuit and corrosion parameters for AZ91D alloy after 2 h immersion in 30% ethylene glycol solution with different concentrations of Cl⁻ or F⁻ ions

$C_{\text{paracetamol}}$	R_s	R	C	W	i_{corr}	E_{corr}	IE
mM	($k\Omega \text{ cm}^2$)	($k\Omega \text{ cm}^2$)	($\mu\text{F cm}^{-2}$)	$k\Omega \text{ cm}^2 \text{ s}^{-1/2}$	($\mu\text{A cm}^{-2}$)	V	%
0.01	0.33	6.1	2.7	2.90	0.100	-1.37	80.0
0.05	0.37	10.0	2.2	1.84	0.020	-1.26	96.0
0.1	0.47	8.5	2.4	1.39	0.040	-1.41	92.1
0.5	0.64	5.6	2.8	2.52	0.045	-1.44	91.0
1.0	0.92	5.1	3.6	1.46	0.051	-1.46	89.8

Table 3. Equivalent circuit and corrosion parameters for AZ91D alloy after 2 h immersion in 30% ethylene glycol solution with different concentrations of paracetamol

Generally, the impedance response is well simulated by the classic parallel resistor capacitor (RC) combination in series with the solution resistance (R_s). In this model [10] a charge transfer resistance (R) is in parallel with the double layer capacitance (C), as shown in Figure 4a. Figure 4b is one time constant model containing Warburg impedance (Z_w) in series to R [13], which is related to ion diffusion through passive film and indicates that the corrosion mechanism is controlled not only by a charge-transfer process but also by a diffusion process. The appropriate equivalent model for the impedance diagrams with two time constants, consists of two series circuits, $R_1 Z_w C_1$ and $R_2 C_2$ parallel combination and both are in series with R_s . C_1 is the capacitance of the outer layer, C_2 pertains to the inner layer, while R_1 and R_2 are the respective resistances of the outer and inner layers constituting the surface film, respectively [14]. A linear region at the lower frequencies in the Nyquist plot in Figure 3b would be related to diffusion phenomena [15, 16] thereby an equivalent circuit with Warburg component Z_w is more appropriate. Analysis of the experimental spectra were made by best fitting to the corresponding equivalent circuit using Thales software provided with the workstation where the dispersion formula suitable to each model was used [14]. In this complex formula an empirical exponent (α), varying between 0 and 1, is introduced to account for the deviation from the ideal capacitive behavior due to surface inhomogeneties, roughness factors and adsorption effects [10]. An ideal capacitor corresponds to $\alpha=1$ while $\alpha=0.5$ becomes the CPE in a Warburg component [17]. In all cases, good conformity between theoretical and experimental results was obtained for the whole frequency range with an average error of 5%.

The effect of concentration for ethylene glycol or additive ions or inhibitor on the relative thickness ($1/C_T$) [18] of AZ91D. Figure 5 reveals features generally concurrent to the behavior of the film resistance. It shows that the resistance (R_T) and the relative thickness ($1/C_T$) of the surface film on AZ91D sample increase with increasing the concentration of ethylene glycol. Thus, 30% ethylene glycol (blank) is an aggressive solution as shown in SEM image in Fig. 6a, where corrosion products appear on the surface. Pure ethylene glycol has very poor electrical conductivity and is almost an insulator [7]. However, dilution by water facilitates the hydrolysis of the hydroxyl groups in ethylene glycol increasing its electrical conductivity. Ethylene glycol molecule is larger than water, so the adsorption of the former at the surface of AZ91D alloy can result in a lower capacitance value [7]. When the concentration of ethylene

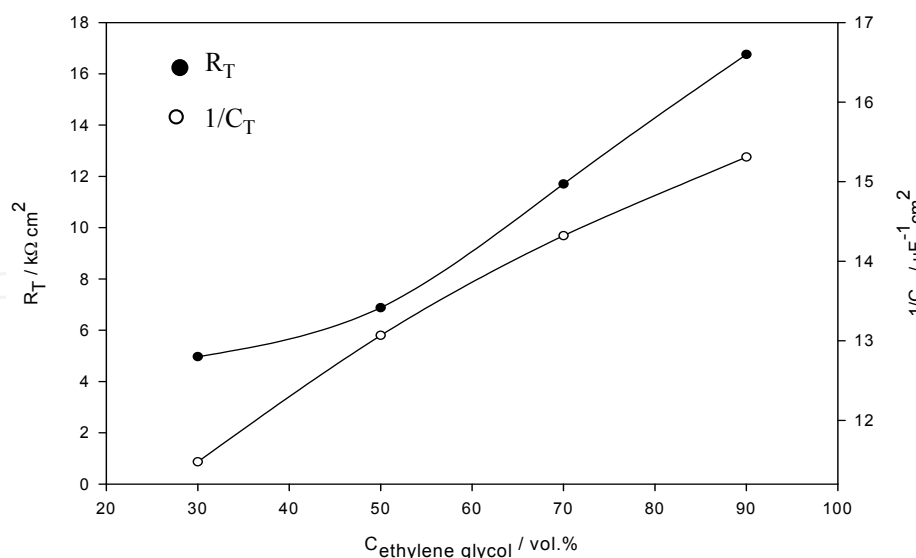


Figure 5. The total resistance (R_T) and relative thickness ($1/C_T$) for AZ91D alloy at various concentrations of ethylene glycol solution, measured after 2 h immersion.

glycol increases, more ethylene glycol will be adsorbed on the surface, leading to a lower C_T . This explains the decreasing corrosion rate of AZ91D alloy with increasing concentration of ethylene glycol and also the decrease in the Warburg impedance diffusion.

As given in Table 2, in ethylene glycol solution contaminated with chloride ions, the resistance decreases sharply at first then reaches a quasi state value with increasing concentration of contaminant [6]. The addition of chloride does not significantly increase the capacitance value until the amount of the added Cl^- ions is above a certain level ($> 0.05 \text{ M}$). At concentrations $> 0.05 \text{ M}$, they are more corrosive than the blank, indicating film dissolution, which can be attributed to the more aggressive nature of the chloride anion. The increase in capacitance should be due to the replacement of ethylene glycol on the alloy surface by the chloride ions as contaminant.

Fluoride is also an important substance that could exist in normal water and can easily be introduced into vehicle coolant systems [19]. As given in Table 2, in fluoride medium at concentrations $> 0.05 \text{ M}$, R and $1/C$ of the surface film increase steeply than the blank due to the formation of less soluble and more stable magnesium fluoride (MgF_2) film [17]. This is confirmed by SEM micrograph of 0.3 M fluoride in ethylene glycol concentration (Figure 6b), the grain particles of the salt film grow laterally during the prolonged exposure (2 h) covering nearly the whole surface of the alloy indicating more stability as compared to the blank shown in Figure 6a. In fact, F has recently been used as an inhibitor in coolants for magnesium alloys [7]. However, the inhibition mechanism has not been systematically studied. Gulbrandsen et. al. [20] reported that crystalline KMgF_3 was identified on magnesium at higher F concentration in the more alkaline solutions. At 0.01 M fluoride concentration ethylene glycol may help in the formation of this compound, so that the resistance decreases than the blank. Table 2 shows that the addition of F into ethylene glycol strikingly enhanced

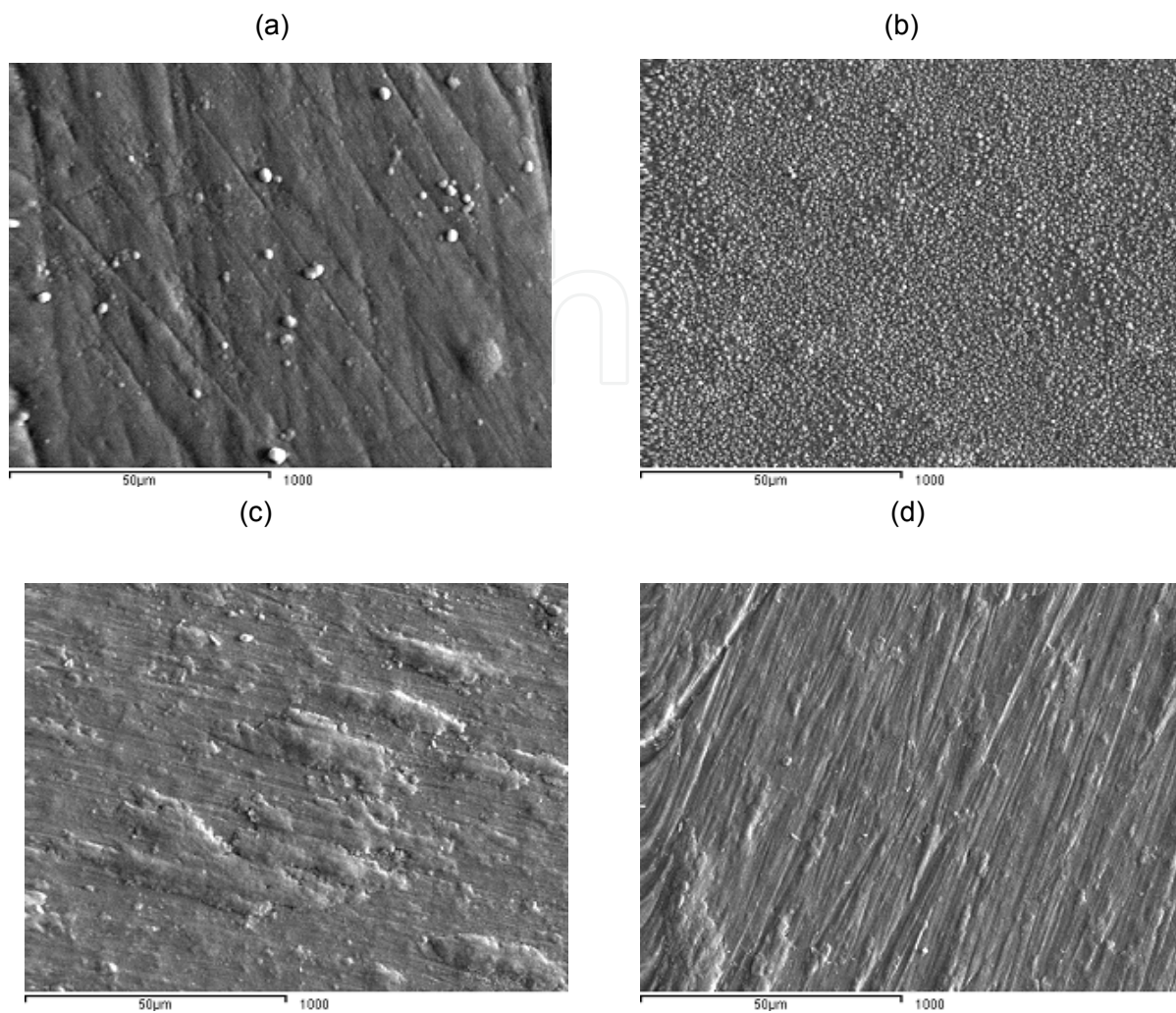


Figure 6. (a-d). SEM micrograph of the (a) blank (30% ethylene glycol solution), (b) 0.3 M F⁻ (c) 0.05 mM paracetamol and (d) 1.0 mM paracetamol, ethylene glycol containing solution.

R but decreased R_s and C. The significantly reduced C and dramatically improved R suggest that [7] a three-dimensional film was formed on the magnesium surface which is much thicker than the adsorbed film and thus can effectively separate the magnesium alloy from the solution, making the corrosion reaction at the interface very slow. As to the solution resistance R_s , its decrease after the addition of F⁻ can be simply attributed to the increased total concentration of ions by adding F into the solution.

Finally, the effect of adding paracetamol as inhibitor was studied; it was found that all concentrations give good inhibition as compared to the blank which may be due to the adsorption of the inhibitor through the adsorption. The rate of adsorption is usually rapid and hence, the reactive metal surface is shielded from the aggressive environment [21]. However, it was found that there is a critical concentration for the inhibitor at 0.05 mM which has the highest resistance as shown in Table 3, and the resistance decreases with increasing the inhibitor concentration > 0.05 mM. This behavior is confirmed by SEM micrographs shown in

Figure 6(c,d), where Figure 6c is for 0.05 mM and Figure 6b for 1.0 mM paracetamol containing ethylene glycol solution. Figure 6c shows a denser and smoother film adsorbed on the alloy surface than that formed on 1.0 mM concentration Figure 6d, Also the two are much better than the blank shown in Figure 6a.

5.2. Potentiodynamic polarization measurements

5.2.1. AZ91D alloy in ethylene glycol solution [6]

The anodic and cathodic (E-log i) plots of AZ91D alloy in the ethylene glycol solution of different concentrations were also studied using potentiodynamic polarization measurements at a scan rate of 1.0 mV s⁻¹. The curves were swept from -2.5 V to -1.0 V vs. SCE. Prior to the potential scan the electrode was left for 2 h until a steady free corrosion potential (E_{st}) value was recorded. The electrochemical parameters shown in Tables 1 and 2 were obtained by analyzing the I/E data as described elsewhere [10]. The corrosion potential (E_{corr}) and current density (i_{corr}) were calculated by Tafel extrapolation method for the cathodic branches of the polarization curves. Furthermore, to illustrate the relative stability of the surface film on AZ91D alloy in the investigated solutions, i_{corr} values are found to decrease and E_{corr} values shifts positively with increasing ethylene glycol percentage. Since increasing water percentage in ethylene glycol is responsible for the corrosivity of the solution to the alloy. However, in chloride containing solution i_{corr} values increases and E_{corr} values shifts to more negative values with increasing Cl concentration. This behavior reflects the harmful influence of Cl ions on the corrosion performance of AZ91D in aqueous liquids [7]. In Fluoride containing solutions, a strange behavior occurs, where i_{corr} decreases and E_{corr} values tend to more negative values with increasing F concentration. Particularly, the role of the β-phase in corrosion is extensively addressed for AZ91D, and it is generally accepted that the β-phase is a corrosion barrier and its presence in an AZ91D alloy is beneficial to the corrosion resistance of the alloy. The reason is fluoride refined AZ91D magnesium alloy by blocking the growth of primary fir-tree crystals in the crystal boundary [22]. Thus, the dimension of β phase is decreased. In the cathodic reaction process, the overpotential of the hydrogen generation increased due to the dispersion of β phase, which resulted in the corrosion potential of the AZ91D.

Fig. 7 shows polarization scans for paracetamol, from which i_{corr} values is calculated and drawn against inhibitor concentration (Fig. 8). As can be seen, i_{corr} value is the lowest at 0.05 mM paracetamol concentration, which is a critical concentration and shows the highest inhibition efficiency (IE) of 96% which calculated from the following equation:

$$IE \% = 1 - \frac{i_{inh}}{i_{corr}} \times 100 \quad (1)$$

Generally, impedance and polarization measurements confirm each other and all are confirmed by SEM images.

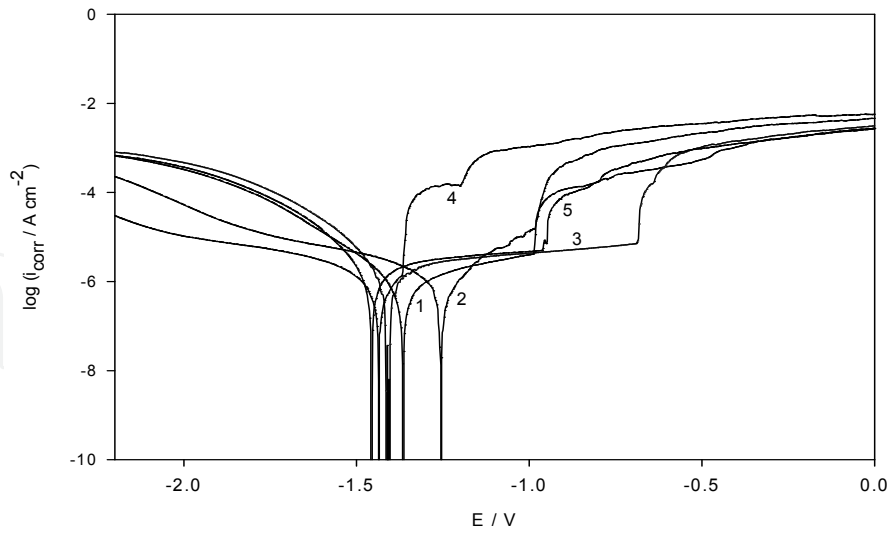


Figure 7. Cathodic and anodic scans of AZ91D alloy exposed after 2 h immersion in 30% ethylene glycol solution with paracetamol of various concentrations: (1) 0.01 mM, (2) 0.05 mM, (3) 0.1 mM, (4) 0.5 mM and (5) 1.0 mM.

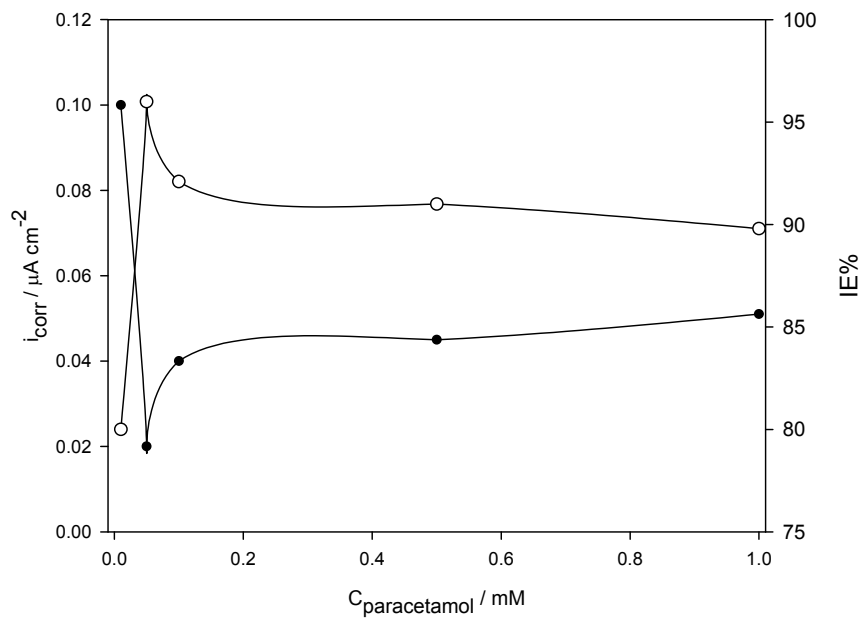


Figure 8. Variation of i_{corr} and IE% for AZ91D alloy exposed after 2 h immersion in 30% ethylene glycol solution with various concentrations of paracetamol.

5.2.2. AZ31E alloy in oxalic acid solution [12]

The impedance measurements recorded after 2 hours of immersion for AZ31E electrode in oxalic acid solution with different concentrations are presented in Figure 9. Bode plots show an intermediate frequency phase peak shifts to lower frequency and higher phase angle

maximum with decreasing oxalic acid concentration. Also, impedance values increase with decreasing the concentration of oxalic acid. The appropriate equivalent model used (Figure 4c) consists of two circuits in series from $R_1C_1Z_W$ and R_2C_2 parallel combination and both are in series with R_s as discussed above. In all cases, good conformity between theoretical and experimental results was obtained with an average error of 4%. The evaluated experimental values are given in Table 4.

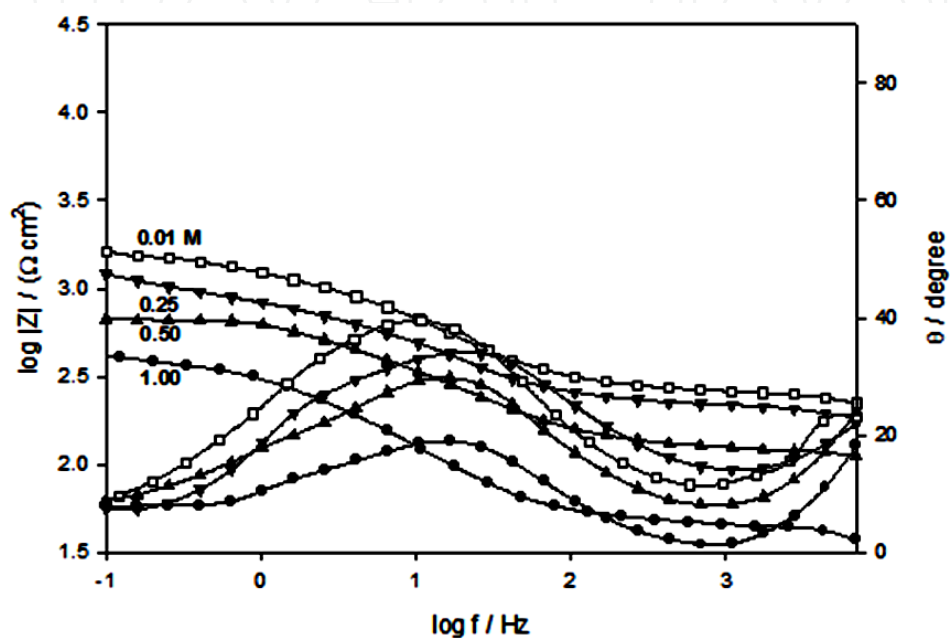


Figure 9. Bode plots of AZ31E electrode in naturally aerated oxalic acid solution of different concentrations, at 298 K.

$\text{Na}_2\text{C}_2\text{O}_4$	R_1	C_1	α_1	R_2	W	C_2	α_2	R_s
M	$\text{k}\Omega \text{ cm}^2$	$\mu\text{F cm}^{-2}$		$\Omega \text{ cm}^2$	kDW	$\mu\text{F cm}^{-2}$		$\Omega \text{ cm}^2$
0.01	2.1	4.7	0.94	58.3	10.2	19.2	0.58	243
0.25	1.3	5.4	0.93	35.6	9.7	20.1	0.56	200
0.50	0.8	6.6	0.91	22.3	7.5	21.3	0.55	100
1.00	0.7	8.3	0.90	14.4	5.2	22.0	0.52	44

Table 4. Impedance parameters of AZ31E electrode in naturally aerated oxalic acid of different concentrations, at 298 K.

It was found that, when AZ31E electrode was immersed in oxalic acid solution, two competitive processes occur. The first one is oxide formation which yields a compact magnesium oxide film with good corrosion resistance. The second one is the formation of magnesium oxalate complexes, which yields a thick porous film as in case of Aluminum alloys [23] with expected

low corrosion resistance, where oxalate ions are bidentate ligands capable of forming strong surface complexes. With increasing of oxalic acid concentration the alternation of the compact oxide film by porous one will increase leading to an increase in the corrosion rate. This also is due to increasing of the acidity of the medium.

In Table 4, R_1 represents the resistance of the passive film which decreases with increasing of oxalic acid concentration due to alternation of compact film by porous one. Consequently, the decrease in the relative thickness of the passive film ($1/C_1$) supports this concept. As the most stable formula for magnesium oxalate is dehydrated one [24], so R_2 can represent the resistance of the hydrated layer and the decreasing of relative thickness ($1/C_2$) of this layer with increasing of oxalic acid concentration reflects the strong adsorption of the oxalate anion with increasing of its concentration and increasing of hydrogen evolution. Moreover, the presence of diffusion process at the interfacial layer of the electrode indicates again the formation of porous film and the decreasing of diffusion impedance indicating the increase of electrolyte diffusion through the pores, as a sequence of increasing of the porosity with the increase of oxalate concentration.

At the lowest concentration of oxalic acid (0.01 M) with highest corrosion resistance, the tested electrode was immersed in this solution containing either Cl^- , F^- or PO_4^{3-} ions with various anion concentrations (0.01 to 1.0 M). Figures 10 and 11 show Bode plots as examples for Cl^- and PO_4^{3-} ions, respectively. The EIS results of the tested electrode were analyzed, following the suitable proposed model in Figure 4c.

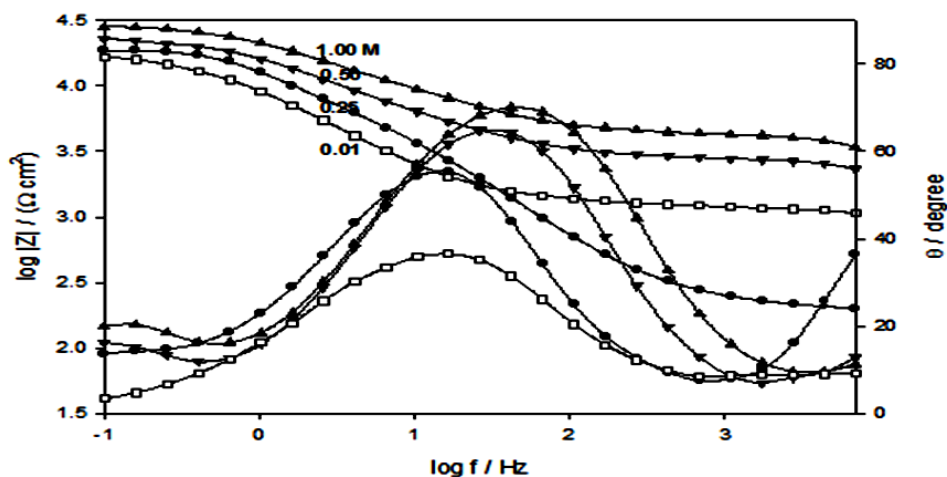


Figure 10. Bode plots of AZ31E electrode as a function of concentration for Cl^- anion in naturally aerated 0.01 M oxalic acid solution, at 298 K.

The theoretical simulated parameters for the tested alloy at each concentration from the added anions (Cl^- , F^- or PO_4^{3-}) to the forming 0.01 M oxalic acid solution were computed and summarized in Table 5.

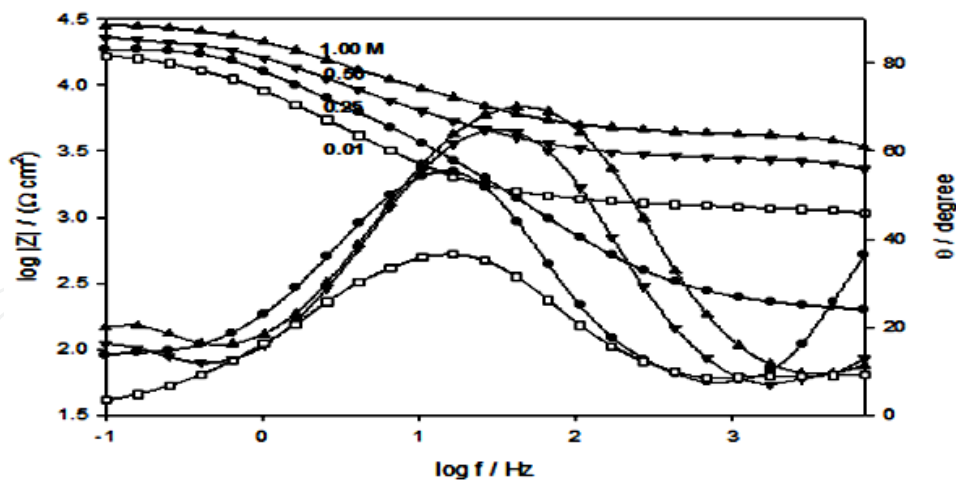


Figure 11. Bode plots of AZ31E electrode as a function of concentration for PO_4^{3-} anion in naturally aerated 0.01 M oxalic acid solution, at 298 K.

Anion	C	R_1	C_1	α_1	R_2	W	C_2	α_2	R_s	i_{corr}
	M	$\text{K}\Omega \text{ cm}^2$	$\mu\text{F cm}^{-2}$		$\Omega \text{ cm}^2$	kDW	nF cm^{-2}		$\Omega \text{ cm}^2$	$\mu\text{A cm}^{-2}$
Cl^-	blank	2.10	4.7	0.84	58.3	10.2	19.2	0.58	243	31.7
	0.01	20.0	2.5	0.83	94.1	5.30	7.60	0.57	501	13.4
	0.25	14.3	2.9	0.83	87.4	4.30	11.9	0.56	80	16.7
	0.50	10.5	3.9	0.81	82.1	3.10	14.9	0.54	100	20.6
	1.00	6.70	4.1	0.84	63.7	1.50	18.6	0.53	589	25.1
F^-	blank	2.10	4.7	0.84	58.3	10.2	19.2	0.58	243	31.7
	0.01	23.8	2.1	0.81	110	9.30	5.30	0.59	208	10.8
	0.25	21.3	2.5	0.87	106	8.60	6.40	0.67	80	11.2
	0.50	18.6	2.6	0.87	91.6	7.50	9.60	0.62	100	12.1
	1.00	15.8	2.8	0.81	69.2	6.70	10.1	0.59	589	14.0
PO_4^{3-}	Blank	2.10	4.7	0.84	58.3	10.2	19.2	0.58	243	31.7
	0.01	17.0	2.4	0.87	121	4.20	7.40	0.57	1075	30.0
	0.25	20.1	2.1	0.88	143	5.40	6.10	0.52	199	15.8
	0.50	24.2	1.2	0.85	165	6.20	5.60	0.56	2290	3.50
	1.00	28.9	0.6	0.82	198	8.10	4.70	0.65	3388	2.41

Table 5. Impedance and corrosion parameters of AZ31E electrode as a function of concentration for Cl^- , F^- and PO_4^{3-} anions in naturally aerated 0.01 M oxalic acid, at 298 K.

In chloride or fluoride additive solutions, the total resistance (Figure 12), Warburg resistance and $1/C$ decreases with increasing its concentrations. As stated previously, this is due to the

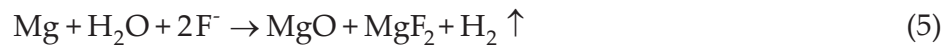
deleterious effect of chloride ions [10]. For F ions, an oxidation reaction occurred in the formation of MgF_2 as follows:



Since $\text{Mg}(\text{OH})_2$ was not stable in acidic solution [25], reactions should occur as follows:



The overall reaction occurred as follows:



The pores in the film should be generated by the hydrogen evolution. These pores might be decreased or filled by the precipitation of MgF_2 particles [25], thus the presence of fluoride ions decreases the corrosion of the tested alloy than the blank (0.01 M oxalic acid). However, depassivation process occurs by increasing fluoride concentration due to breakdown of the formed grained layer of MgF_2 that leads to drastic increase in the surface roughness. Furthermore, in presence of F ions, aluminum which becomes enriched in the surface can form the soluble complex $(\text{AlF}_6)^{3-}$, thereby, participates at higher F ions concentrations in decreasing the stability of the passive surface film on AZ31E alloy [14]. However, Cl ion is more strongly adsorbed on the alloy surface than F ions, so, its resistivity is lower than fluoride ion.

For phosphate anion as additive, increasing the total resistance (R_T) (Figure 12), W and $1/C_1$ with increasing of phosphate concentration indicates that interaction between oxalic acid and phosphate forms phosphate complexes that increase with increasing phosphate concentration and leads to passivation of AZ31E surface. Also, by measuring the pH of the medium, it increases slightly from acidic ~ 6.8 to basic medium reaching to 11.1 at 1.0 M phosphate concentration, leading to passivation. At pH 11.1, HPO_4^{2-} species has almost equal tendency for existing in solution as PO_4^{3-} anions and thus the solution at this pH will contain the two phosphate species with nearly equal relative fraction [2, 26-27]. Therein the electrolyte pH plays a determinant influence on film properties, where films formed in phosphate solutions at higher pH values are thicker of better protection for the alloy than those formed in acidic ones.

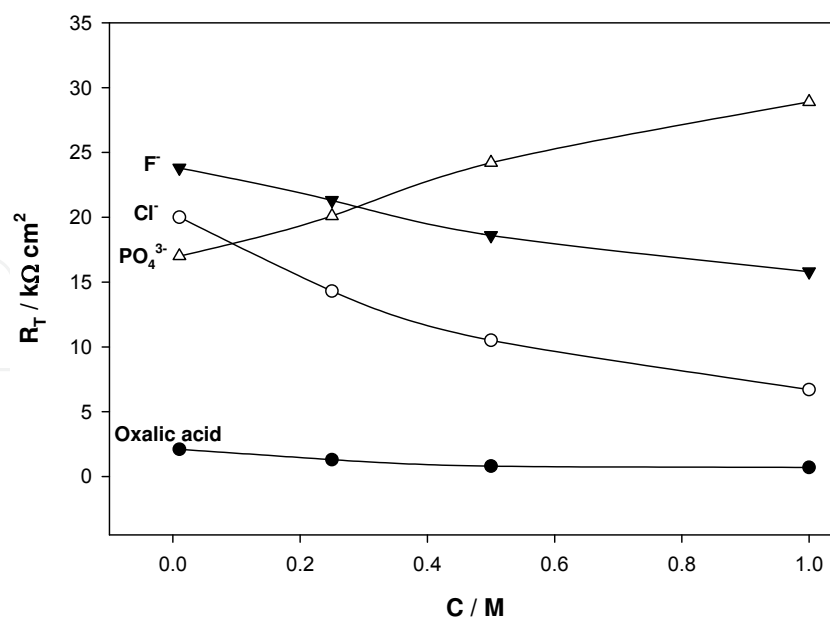


Figure 12. Variation of R_T of AZ31E electrode as a function of concentration for oxalic acid and Cl^- , F^- or PO_4^{3-} anions in naturally aerated 0.01 M oxalic acid solution, at 298 K.

Impedance results are in good agreement with polarization data.

5.2.3. AZ31E alloy in oxalic acid solution [12]

The Potentiodynamic polarization behavior of the AZ31E electrode was studied in relation to concentration of oxalic acid electrolyte. Figure 13 shows the scans for the tested electrode in 0.01 M oxalic acid solution with different concentrations (0.01-1.0 M) of PO_4^{3-} ion, at a scan rate of 1 mV/s over the potential range from -2.0 to 1.0 V vs. SCE. Prior to the potential sweep, the electrode was left for 2 hours until a steady state potential was reached.

On increasing the concentration of oxalic acid, an increase in the corrosion current density was observed (Figure 14). This may reflect the changing of the nature of the film formed on the surface (may represent the replacement of MgO by $\text{Mg}_2\text{C}_2\text{O}_4$).

The effect of added Cl^- or F^- or PO_4^{3-} ions on the electrochemical behavior of the tested AZ31E electrode in 0.01 M $\text{H}_2\text{C}_2\text{O}_4$ solution at 298 K is shown in Figure 15. It was found that i_{corr} value increases with increasing either Cl^- or F^- ion concentration reflecting the harmful effect of both ions leading to an increase in hydrogen evolution [28-29] and corrosion rate. For phosphate ion, i_{corr} value decreases with increasing its concentration that is the corrosion rate decreases. So, phosphate is useful in reducing the corrosion or hydrogen evolution rate [30-31]. These results coincide with that drawn from EIS data.

Generally, for comparing corrosion rate obtained from Tafel and EIS measurements, it is well known that the polarization resistance R_p is related to the corrosion rate through Tafel slopes β_a and β_c by Stern–Geary equation [32]:

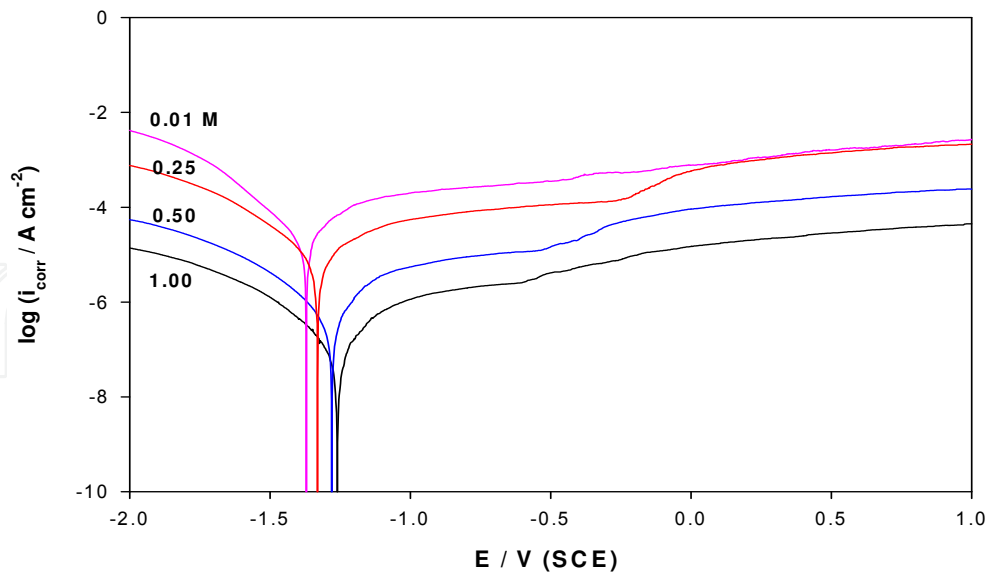


Figure 13. Potentiodynamic polarization scans of AZ31E electrode as a function of concentration for PO_4^{3-} anion in naturally aerated 0.01 M oxalic acid solution, at 298 K.

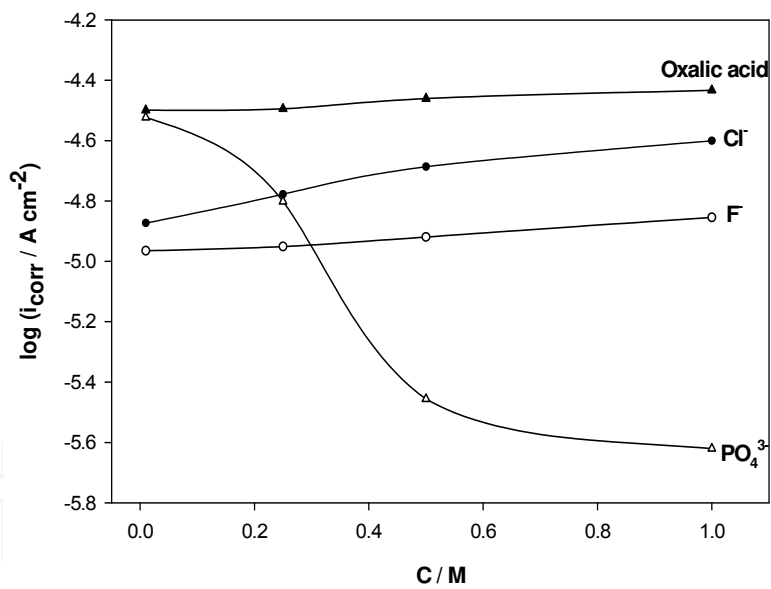


Figure 14. Variation of logarithm of corrosion current density (i_{corr}) for AZ31E electrode as a function of concentration for oxalic acid and Cl^- , F^- or PO_4^{3-} anions in naturally aerated 0.01 M oxalic acid solution, at 298 K.

$$i_{corr} = \frac{1}{2.303R_p \left(\frac{1}{\beta_a} + \frac{1}{|\beta_c|} \right)} \quad (6)$$

Anion	C	R _T	i _{corr} (EIS)	P _i (EIS)	i _{corr} (Tafel)	R _p	P _i (Tafel)
	M	KΩ cm ²	μA cm ⁻²	mm/y	μA cm ⁻²	kΩ cm ²	mm/y
Cl ⁻	blank	2.10	109.4	2.50	31.7	7.24	0.72
	0.01	20.0	14.28	0.33	13.4	21.3	0.31
	0.25	14.3	19.41	0.45	16.7	16.7	0.38
	0.50	10.5	26.16	0.59	20.6	13.4	0.47
	1.00	6.70	41.1	0.93	25.1	10.9	0.57
F ⁻	blank	2.10	109.43	2.50	31.7	7.24	0.72
	0.01	23.8	18.93	0.43	10.8	41.5	0.25
	0.25	21.3	21.44	0.49	11.2	40.8	0.26
	0.50	18.6	25.57	0.58	12.1	39.5	0.28
	1.00	15.8	27.07	0.62	14.0	30.6	0.32
PO ₄ ³⁻	blank	2.10	109.43	2.50	31.7	7.24	0.72
	0.01	17.0	41.98	0.96	30.0	23.8	0.69
	0.25	20.1	32.36	0.74	15.8	41.2	0.36
	0.50	24.2	8.391	0.19	3.50	58.1	0.08
	1.00	28.9	5.883	0.13	2.41	70.8	0.06

Table 6. Corrosion rate (P_i) calculated from EIS and Tafel methods of AZ31E electrode as a function of concentration for Cl⁻, F⁻ and PO₄³⁻ anions in naturally aerated 0.01 M oxalic acid, at 298 K.

As given in Table 6, it can be seen that evaluated R_p values obtained from Tafel measurements have the same trend as R_T obtained from EIS measurements. By calculating i_{corr} from EIS measurements using cathodic, anodic slopes and R_T, it was found that they also have the same trend as that obtained from Tafel measurements. By calculation of corrosion rate, where i_{corr} (mA cm⁻²) is related to the average corrosion rate in mm/y (P_i) using [4]:

$$P_i = 22.85i_{\text{corr}} \quad (7)$$

It was found that corrosion rate obtained from EIS method is comparable with that obtained from Tafel extrapolation method. Thus there is a good agreement between corrosion rates determined by both techniques.

6. Conclusions

The corrosion rate of magnesium alloy in aqueous ethylene glycol depends on the concentration of the solution. A diluted ethylene glycol solution is more corrosive than a concentrated

one at room temperature. Ethylene glycol solution containing $\text{Cl}^- > 0.05 \text{ M}$ or $\text{F}^- < 0.05 \text{ M}$ are more corrosive than the blank (30% ethylene glycol-70% water). However, at concentrations < 0.05 for chloride or $> 0.05 \text{ M}$ fluoride ions, some inhibition effect has been observed. The corrosion of AZ91D alloy in the blank can be effectively inhibited by addition of 0.05 mM paracetamol that reacts with AZ91D alloy and forms a protective film on the surface at this concentration.

The corrosion rate of AZ31E magnesium alloy in oxalic acid solution depends on the concentration of the solution and the additive. A concentrated oxalic acid solution with lowest pH and highest hydrogen evolution is the more corrosive one. Oxalic acid solution of 0.01 M concentration containing Cl^- or F^- are more corrosive with increasing the concentration from 0.01 to 1.0 M for the anions as observed from impedance or polarization techniques. For PO_4^{3-} anion in 0.01 M oxalic acid solution, it acts passivator. The corrosion rate decreases with increasing its concentration.

Author details

Amany Mohamed Fekry

Cairo University (Faculty of Science, Chemistry Department), Egypt

References

- [1] Fekry A., Electrochemical Corrosion Behavior of Magnesium Alloys in Biological Solutions, In Czerwinski F. (Ed.), Magnesium Alloys-Corrosion and Surface Treatments. Rijeka: InTech; 2011. p 65-92.
- [2] Heakal F, Fekry A, Fatayerji M. Electrochemical behavior of AZ91D magnesium alloy in phosphate medium-Part I. Effect of pH. J. Applied Electrochemistry 2009;39(5) 583-591.
- [3] Zhang T, Liu X, Shao Y, Meng G, Wang F. Electrochemical noise analysis on the pit corrosion susceptibility of Mg-10Gd-2Y-0.5Zr, AZ91D alloy and pure magnesium using stochastic model. Corrosion Science 2008; 50(12) 3500-3507.
- [4] Song G, Bowles A, StJohn D. Corrosion resistance of aged die cast magnesium alloy AZ91D. Materials Science and Engineering 2004;A366(1) 74-86.
- [5] Song G, Atrens A, Dargusch M. Influence of microstructure on the corrosion of die-cast AZ91D. Corrosion Science 1998;41(2) 249-273.
- [6] Fekry A, Fatayerji M. Electrochemical Corrosion Behavior of AZ91D Alloy in Ethylene Glycol. Electrochimica Acta 2009;54(26) 6522-6528.

- [7] Song G, StJohn D, Corrosion behaviour of magnesium in ethylene glycol Original Research Article *Corrosion Science* 2004 46(6) 1381-1399.
- [8] Song G. Corrosion and its inhibition of engine block magnesium alloys in coolants, CAST Report 2001081, 2001 (confidential).
- [9] PCT/IB99/01659, 1999.
- [10] Fekry A. The influence of chloride and sulphate ions on the corrosion behavior of Ti and Ti-6Al-4V alloy in oxalic acid. *Electrochimica Acta* 2009;54(12) 3480-3489.
- [11] Maruthamuthu P, Ashokkumar M. Hydrogen generation using Cu(II)/WO₃ and oxalic acid by visible light. *International Journal of Hydrogen Energy* 1988;13(11) 677-680.
- [12] Fekry A. Impedance and hydrogen evolution studies on magnesium alloy in oxalic acid solution containing different anions. *International journal of Hydrogen Energy* 2010; 35(23) 12945-12951.
- [13] Beccaria A, Bertolotto C. Inhibitory action of 3-trimethoxysilylpropanethiol-1 on copper corrosion in NaCl solutions. *Electrochimica Acta* 1997; 42(9) 1361-1371.
- [14] Heakal F, Fekry A, Fatayerji M. Influence of halides on the dissolution and passivation behavior of AZ91D magnesium alloy in aqueous solutions. *Electrochimica Acta* 2009;54(5) 1545-1557.
- [15] Macdonald J, In Macdonald J. (Ed.), *Emphasizing Solid Materials and Systems*. John Wiley & Sons, 1987.
- [16] Macdonald D. Reflections on the history of electrochemical impedance spectroscopy. *Electrochimica Acta* 2006 51(8-9) 1376-1388.
- [17] Retter U, Widmann A, Siegler K, Kahlert H. On the impedance of potassium nickel(II) hexacyanoferrate(II) composite electrodes—the generalization of the Randles model referring to inhomogeneous electrode materials. *Journal of Electroanalytical Chemistry* 2003;546, 87-96.
- [18] Heakal F, Fekry A. Experimental and Theoretical Study of Uracil and Adenine Inhibitors in Sn-Ag Alloy/Nitric Acid Corroding System. *Journal of Electrochemical Society* 2008;155(11) C534-542.
- [19] Song G, Atrens A, Wu X, Zhang B. Corrosion behaviour of AZ21, AZ501 and AZ91 in sodium chloride. *Corrosion Science* 1998;40(10) 1769-1791.
- [20] Gulbrandsen E, Tafto J, Olsen A. The passive behaviour of Mg in alkaline fluoride solutions. *Electrochemical and electron microscopical investigations*. *Corrosion Science* 1993;34(9) 1423-1440.
- [21] Chao C, Lin L, Macdonald D. Point defect model for anodic passive films, *Journal of Electrochemical Society* 1981;128(6) 1181-1187.

- [22] Liu Y, Wang Q, Song Y, Zhang D, Yu S, Zhu X. A study on the corrosion behavior of Ce-modified cast AZ91 magnesium alloy in the presence of sulfate-reducing bacteria. *Journal of Alloys and Compounds* 2009;473(1-2) 550-556.
- [23] Jain AK, Acharya NK, Kulshreshtha V, Awasthi K, Singh M, Vijay YK. Study of hydrogen transport through porous aluminum and composite membranes. *International Journal of Hydrogen Energy* 2008;33(1) 346-349.
- [24] Fekry A, El-Sherief R. Electrochemical corrosion behavior of Magnesium and Titanium alloys in simulated body fluid. *Electrochimica Acta* 2009;54(28) 7280-7285.
- [25] Ma L, Wang P, Cheng H. Hydrogen sorption kinetics of MgH_2 catalyzed with titanium compounds. *International Journal of Hydrogen Energy* 2010;35(7) 3046-3050.
- [26] Heakal F, Fekry A, Fatayerji M. Electrochemical behavior of AZ91D magnesium alloy in phosphate medium—Part II. Induced passivation. *Journal of Applied Electrochemistry* 2009;39(9)1633-1642..
- [27] Muñoz L, Bergel A, Féron D, Basséguy R. Hydrogen production by electrolysis of a phosphate solution on a stainless steel cathode. *International Journal of Hydrogen Energy* 2010;35(16) 8561-8568.
- [28] Uan JY, Cho CY, Liu KT. Generation of hydrogen from magnesium alloy scraps catalyzed by platinum-coated titanium net in NaCl aqueous solution. *International Journal of Hydrogen Energy* 2007;32(13) 2337-2343.
- [29] Ameer M, Fekry A. Inhibition effect of newly synthesized heterocyclic organic molecules on corrosion of steel in alkaline medium containing chloride. *International Journal of Hydrogen Energy* 2010;35(20) 11387-11396.
- [30] Fekry A, Ameer M. Corrosion inhibition of mild steel in acidic media using newly synthesized heterocyclic organic molecules. *International Journal of Hydrogen Energy* 2010;35(14) 7641-7651.
- [31] Azizi O, Jafarian M, Gobal F, Heli H, Mahjani MG. The investigation of the kinetics and mechanism of hydrogen evolution reaction on tin. *International Journal of Hydrogen Energy* 2007;32(12)1755-1761.
- [32] Boudjemaa A, Boumaza S, Trari M, Bouarab R, Bouguelia A. Physical and photo-electrochemical characterizations of $\alpha\text{-Fe}_2\text{O}_3$. Application for hydrogen production. *International Journal of Hydrogen Energy* 2009;34(10) 4268-4274.